

Modeling of chaotic motion of gyrostats in resistant environment on the base of dynamical systems with strange attractors

Anton V. Doroshin*

S.P. Korolev Samara State Aerospace University (National Research University), Russia.

Abstract. A chaotic motion of gyrostats in resistant environment is considered with the help of well known dynamical systems with strange attractors: Lorenz, Rössler, Newton-Leipnik and Sprott systems. Links between mathematical models of gyrostats and dynamical systems with strange attractors are established. Power spectrum of fast Fourier transformation, gyrostat longitudinal axis vector hodograph and Lyapunov exponents are find. These numerical techniques show chaotic behavior of motion corresponding to strange attractor in angular velocities phase space. Cases for perturbed gyrostat motion with variable periodical inertia moments and with periodical internal rotor relative angular moment are considered; for some cases Poincaré sections are obtained.

Keywords: Rigid Body; Gyrostat; Resistant Environment; Strange Attractors; Lorenz, Rössler, Newton-Leipnik, Sprott Systems; Lyapunov exponents; Fast Fourier Transformation; Poincaré Sections.

MSC2010: 70E17, 34C28, 37D45

1 Introduction

Problem of rigid bodies motion and its practical engineering applications such as gyroscopes, gyrostats and dual-spin-spacecraft are very important for modern science. Despite classical analytical research results and exact solutions this problem is still far from complete due to the existence of chaos phenomena [1-13]. Among the basic directions of modern research within the framework of the indicated problem it is possible to highlight the following points: deriving exact and approximated analytical and asymptotic solutions, investigation into stability of motion, the analysis of motion under an influence of external regular and stochastic disturbance, research into dynamic chaos and study of non-autonomous systems with variable parameters.

Recently, chaotic dynamic has becomes one of the major part of nonlinear science. Applications of dynamical systems with chaotic behavior and strange attractors are seen in many areas of science, including space-rocket systems [7-12]. E. N. Lorenz and O. E. Rössler systems [1, 2] represent classical dynamical systems with strange attractors. R. B. Leipnik and T. A. Newton [3] found two strange attractors in rigid body motion. Since Leipnik and Newton's work, the chaotic dynamics of rigid body motion investigates in many works. J. C. Sprott [4, 5] examined 19 systems of three-dimensional autonomous ordinary differential equations with strange attractors; also critical points, Lyapunov exponents and fractional dimensions of systems were found.

Work [7] contains the analysis of chaotic behavior of a spacecraft with periodic time-dependent moments of inertia during its free motion. The equations of variable mass coaxial bodies system were developed in papers [10] where also the attitude motion of coaxial bodies system and double rotation spacecraft with time-dependent moments of inertia were analyzed on

* Correspondence to: A.V. Doroshin, Samara State Aerospace University, SSAU, Moscovskoe shosse 34, Samara, Russia 443086. E-mail: doran@inbox.ru.

the base of special method of phase trajectory curvature analysis. The results [7-12] can be used for the analysis of attitude motion of a gyrostat-satellites and dual-spin spacecraft including motion with an active solid-propellant rocket engine.

In this paper more attention is focused on chaotic attractors in phase space of angular velocity of gyrostat and on perturbed gyrostat motion in resistant environment with energy dissipation/excitation.

Conditions of correspondence of mathematical models of gyrostats in resistant environment and dynamical systems with strange attractors (Lorenz, Rössler, Newton-Leipnik and Sprott) are defined. To confirm the system chaotic behavior numerical computer simulations are used. These simulations are performed by means of numerical integration of the equations of motion with the help of several numerical tools: time history of phase coordinates, gyrostat longitudinal axis vector hodograph, Poincaré map, fast Fourier transform power spectrum. This characterizes the dynamical behavior of the gyrostat in resistant environment as regular or chaotic.

2 Mathematical model

Let us consider a gyrostat attitude motion about fixed point in resistant environment with energy dissipation/excitation (fig.1). Assume resistant environment effect corresponding to action of external forces moments that are constant (\mathbf{M}_{const}^e), linear (\mathbf{M}_{lin}^e) and nonlinear (\mathbf{M}_{quad}^e) in main body angular velocity projections onto body frame axes $x_1x_2x_3$ ($\boldsymbol{\omega} = [p, q, r]^T$).

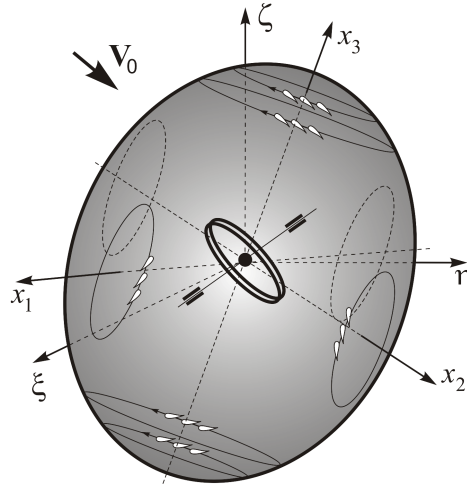


Fig.1 – Inertial ($\xi\eta\zeta$) and gyrostat main body ($x_1x_2x_3$) frames

The motion equations follow from angular moment's law:

$$\dot{\mathbf{K}} + \boldsymbol{\omega} \times (\mathbf{K} + \mathbf{R}) = \mathbf{M}_{const}^e + \mathbf{M}_{lin}^e + \mathbf{M}_{quad}^e \quad (1)$$

where

$$\begin{aligned} \mathbf{K} &= \mathbf{I} \cdot \boldsymbol{\omega}; \quad \mathbf{R} = [R_1, R_2, R_3]^T; \quad \mathbf{M}_{const}^e = [d_1, d_2, d_3]^T; \quad \mathbf{M}_{lin}^e = \mathbf{A} \cdot \boldsymbol{\omega}; \\ \mathbf{M}_{quad}^e &= \mathbf{B} \cdot [p^2, q^2, r^2]^T; \quad \mathbf{A} = [a_{ij}]; \quad \mathbf{B} = [b_{ij}]; \\ a_{ij} &= const; \quad b_{ij} = const; \quad R_i = const; \quad d_i = const; \quad i, j = 1..3 \end{aligned} \quad (2)$$

\mathbf{K} – angular moment of gyrostat main body with “frozen” internal rotor; \mathbf{I} – inertia tensor of main body with “frozen” internal rotor; \mathbf{R} – constant angular moment of relative rotor motion (in

body frame); \mathbf{A} , \mathbf{B} – constant matrixes.

Matrix structure of external forces moments (2) can describe an action of viscous drag, hydro(aero)dynamic lift, nonuniform lift and friction in fluid flow (\mathbf{V}_0) of main body with roughened surface and propeller elements.

Assume coincidence of gyrostat center of mass, rotor center of mass and fixed point. Also let us consider case of spherical inertia tensor of rotor and gyrostat general inertia tensor $\mathbf{I} = \text{diag}(A, B, C)$. In this case scalar form of eq. (1) can be write as follows

$$\begin{cases} A\dot{p} = (B - C)r q + a_{11}p + (a_{12} - R_3)q + (a_{13} + R_2)r + b_{11}p^2 + b_{12}q^2 + b_{13}r^2 + d_1 \\ B\dot{q} = (C - A)p r + a_{22}q + (a_{23} - R_1)r + (a_{21} + R_3)p + b_{21}p^2 + b_{22}q^2 + b_{23}r^2 + d_2 \\ C\dot{r} = (A - B)q p + a_{33}r + (a_{31} - R_2)p + (a_{32} + R_1)q + b_{31}p^2 + b_{32}q^2 + b_{33}r^2 + d_3 \end{cases} \quad (3)$$

Dynamical system (3) is supplemented with kinematical system for Euler type angles (ψ (about x_1) \rightarrow γ (about x_2) \rightarrow φ (about x_3)):

$$\begin{aligned} \dot{\gamma} &= p \sin \varphi + q \cos \varphi; \quad \dot{\psi} = \frac{1}{\cos \gamma} (p \cos \varphi - q \sin \varphi); \\ \dot{\varphi} &= r - \frac{\sin \gamma}{\cos \gamma} (p \cos \varphi - q \sin \varphi). \end{aligned} \quad (4)$$

In considered case gyrostat kinetic energy takes on form:

$$T = \frac{1}{2} (A p^2 + B q^2 + C r^2) + [p R_1 + q R_2 + r R_3] + \frac{1}{2} \{R_1^2 + R_2^2 + R_3^2\} \quad (5)$$

3 Links between gyrostat chaotic motion and strange attractors

It is well known fact that unpredictable chaotic long-term solutions can exist for simple nonlinear deterministic systems. The study of nonlinear dynamics has brought new excitement to one of the oldest fields of science and, certainly, mechanics. So, many papers and, for example, works [3, 11, 12] describe chaotic motion of rigid body and gyrostats as modes corresponded to strange attractors in phase space. The paper [4] also contains several interesting and important chaotic dynamical systems with strange attractors.

In this paper we will find conditions of reduction of gyrostats motion equations (3) to Lorenz, Rössler, Newton-Leipnik and Sprott dynamical systems. General form of indicated dynamical systems of three autonomous first-order ordinary differential equations (ODE) can be write as:

$$\dot{x} = f_x(x, y, z); \quad \dot{y} = f_y(x, y, z); \quad \dot{z} = f_z(x, y, z) \quad (6)$$

The system (6) has strange attractors in many cases including classical dynamical systems, which presented in table 1 [4]. Cases A-S correspond to Sprott systems [4, 5], and LOR, ROS, NL – to Lorenz, Rössler, Newton-Leipnik systems.

It is possible to write condition of equivalence of dynamical systems (3) and A-NL (tabl.1), where variables change take place $\{p \leftrightarrow x, q \leftrightarrow y, r \leftrightarrow z\}$.

First of all we take notice about signature (+/-) in table 1. Signature "+" means possibility of reduction of systems A-NL immediately to system (3): it implies definition of corresponded components values of vectors ($\mathbf{R}, \mathbf{M}_{const}^e$) and matrix ($\mathbf{A}, \mathbf{B}, \mathbf{I}$). Signature "-" means

unrealizability of this reduction without presence of additional special control torque of gyroscopic type in right parts of systems (1) and (3):

$$\mathbf{M}_{control}^{gyro} = \mathbf{G} \cdot [qr, pr, pq]^T; \quad \mathbf{G} = [g_{ij}]; \quad i, j = 1..3 \quad (7)$$

This artificial forces moment (7) can be formed with the help of special technical actuators and thrusters.

Table 1

| Case | f_x | f_y | f_z | Signature |
|------|------------------------------|------------------------|------------------------------|-----------|
| A | y | $-x+yz$ | $1-y^2$ | - |
| B | yz | $x-y$ | $1-xy$ | + |
| C | yz | $x-y$ | $1-x^2$ | - |
| D | $-y$ | $x+z$ | $xz+3y^2$ | - |
| E | yz | x^2-y | $1-4x$ | - |
| F | $y+z$ | $-x+y/2$ | x^2-z | + |
| G | $2x/5+z$ | $xz-y$ | $-x+y$ | - |
| H | $-y+z^2$ | $x+y/2$ | $x-z$ | + |
| I | $-y/5$ | $x+z$ | $x+y^2-z$ | + |
| J | $2z$ | $-2y+z$ | $-x+y+y^2$ | + |
| K | $xy-z$ | $x-y$ | $x+0.3z$ | - |
| L | $y+3.9z$ | $0.9x^2-y$ | $1-x$ | + |
| M | $-z$ | $-x^2-y$ | $1.7(1+x)+y^2$ | + |
| N | $-2y$ | $x+z^2$ | $1+y-2x$ | + |
| O | y | $x-z$ | $x+xz+2.7y$ | - |
| P | $2.7y+z$ | $-x+y^2$ | $x+y$ | + |
| Q | $-z$ | $x-y$ | $3.1+y^2+0.5z$ | + |
| R | $0.9-y$ | $0.4+z$ | $xy-z$ | - |
| S | $-x-4y$ | $x+z^2$ | $1+x$ | + |
| LOR | $-s(x-y)$ $s=10$ | $-y+wx-xz$ $w=28$ | $-vz+xy$ $v=8/3$ | + |
| ROS | $-y-z$ | $x+ky$ $k=0.2$ | $v+(x-w)z$ $v=0.2, w=5.7$ | - |
| NL | $-kx+y+wyz$ $k=0.4, w=10$ | $-x-my+5xz$ $m=0.4$ | $vz-5xy$ $v=0.175$ | - |

Now we can present following conditions of reductions of A-NL systems to system (3), and vice versa. These conditions establish connections between external and internal parameters (mass-inertia, gyrostat rotor angular moment, roughened surface and propeller elements properties, friction in fluid flow etc.).

LOR-case conditions:

$$\begin{cases} A/2 = C = B = B_0; & b_{ij} = d_i = g_{ij} = 0 \\ a_{11} = -2B_0s; & a_{12} = 2B_0s + R_3; & a_{13} = -R_2 \\ a_{21} = B_0w - R_3; & a_{22} = -B_0; & a_{23} = R_1 \\ a_{31} = R_2; & a_{32} = -R_1; & a_{33} = -vC \end{cases} \quad (8.LOR)$$

If we use substitution of coefficient (8.LOR) into system (3), then we obtain classical Lorenz equations.

It is need to note that for LOR-gyrostat ((3) with (8.LOR)) main body is dynamically symmetric ($B=C$) and third inertia moment is twice as large ($A=2B$).

ROS-case conditions:

$$\begin{cases} A = B = C; \quad g_{32} = C; \quad g_{ij}|_{i \neq 3, j \neq 2} = 0; \quad b_{ij} = d_{1,2} = 0; \quad d_3 = \nu C \\ a_{11} = 0; \quad a_{12} = -A + R_3; \quad a_{13} = -A - R_2 \\ a_{21} = B - R_3; \quad a_{22} = kB; \quad a_{23} = R_1 \\ a_{31} = R_2; \quad a_{32} = -R_1; \quad a_{33} = -wC \end{cases} \quad (8.ROS)$$

For ROS-gyrostat spherical inertia-mass symmetry takes place ($A=B=C$).

NL-case conditions:

$$\begin{cases} \forall: A, B, C; \quad b_{ij} = d_i = 0; \quad \mathbf{G} = \text{diag} \\ g_{11} = wA - B + C; \quad g_{22} = 5B + A - C; \quad g_{33} = -5C + B - A \\ a_{11} = -kA; \quad a_{12} = A + R_3; \quad a_{13} = -R_2 \\ a_{21} = -B - R_3; \quad a_{22} = -mB; \quad a_{23} = R_1 \\ a_{31} = R_2; \quad a_{32} = -R_1; \quad a_{33} = \nu C \end{cases} \quad (8.NL)$$

For NL-gyrostat general case of inertia-mass takes place ($A \neq B \neq C$).

A-case conditions:

$$\begin{cases} B = C = A = A_0; \quad g_{21} = A_0; \quad b_{32} = -A_0; \quad d_3 = A_0 \\ a_{11} = 0; \quad a_{12} = A_0 + R_3; \quad a_{13} = -R_2 \\ a_{21} = -B - R_3; \quad a_{22} = 0; \quad a_{23} = R_1 \\ a_{31} = R_2; \quad a_{32} = -R_1; \quad a_{33} = 0 \end{cases} \quad (8.A)$$

where other components of $\mathbf{A}, \mathbf{B}, \mathbf{G}, \mathbf{M}_{const}^e$ equal to zero.

B-case conditions:

$$\begin{cases} A = C; \quad B = 2C; \quad g_{ij} = 0; \quad b_{ij} = 0; \quad d_3 = C \\ a_{11} = 0; \quad a_{12} = R_3; \quad a_{13} = -R_2 \\ a_{21} = B - R_3; \quad a_{22} = -B; \quad a_{23} = R_1 \\ a_{31} = R_2; \quad a_{32} = -R_1; \quad a_{33} = 0 \end{cases} \quad (8.B)$$

F-case conditions:

$$\begin{cases} A = B = C; \quad g_{ij} = 0; \quad b_{31} = 1; \quad d_i = 0 \\ a_{11} = 0; \quad a_{12} = A + R_3; \quad a_{13} = A - R_2 \\ a_{21} = -B - R_3; \quad a_{22} = B / 2; \quad a_{23} = R_1 \\ a_{31} = R_2; \quad a_{32} = -R_1; \quad a_{33} = -C \end{cases} \quad (8.F)$$

Other cases conditions can be write by analogy (by the way of equalization of corresponding coefficients of sys. (3) and A-NL). So we can conclude that dynamical systems with strange attractors A-NL correspond to gyrostats equation ((3) with conditions (8.A), (8.B), (8.NL)...), which allow chaotic modes of motion.

4 Perturbed motion examination

4.1 Inertia moments perturbation

Haw we saw in previous paragraph dynamical system with strange attractors can correspond to system equations of gyrostat motion. Considered gyrostats possessed constant

parameters (moments of inertia, relative rotor angular moment component, resistant environment and gyrostat outer surface properties, etc.). Now let us examine perturbed gyrostat motion with a time-dependent moments of inertia, motion of this gyrostat and influence of parameters variability on strange attractor change. It is need to note, that the inertia moment variability can describe small elastic vibrations in gyrostat construction [7].

LOR-gyrostat.

Assume following time-dependencies of inertia moments in the case of LOR-gyrostat:

$$B(t) = C(t) = B_0(1 + \varepsilon \sin \Omega t); \quad A(t) = 2B_0(1 - \varepsilon \sin \Omega t) \quad (9)$$

where ε is small nondimensional parameter ($0 < \varepsilon < 1$); other parameters in (8.LOR) are constant. Take into account conditions (8.LOR) and dependencies (9) we can write motion equations:

$$\begin{cases} \dot{x} = \frac{-s(x-y)}{1 - \varepsilon \sin \Omega t} \\ \dot{y} = \frac{1}{1 + \varepsilon \sin \Omega t} (wx - y - [1 - 3\varepsilon \sin \Omega t]xz) \\ \dot{z} = \frac{1}{1 + \varepsilon \sin \Omega t} ([1 - 3\varepsilon \sin \Omega t]xy - vz) \end{cases} \quad (10)$$

In order to examine of perturbed motion several numerical techniques are used. They are based on the numerical integration of the equations of motion (10) by means of a Runge–Kutta algorithm. So, we present perturbed strange attractor (fig.2-a) in phase space $\{x, y, z\}$, $x(t)$ time-history (fig.2-b), power spectrum of $x(t)$ fast Fourier transformation (fig.2-c), kinetic energy (5) time-history (fig.2-d), asymptotics of Lyapunov exponents (fig.2-e) and longitudinal axis vector hodograph (fig.2-f). Fig.2 was obtained at $\varepsilon = 0.1$ and $\Omega = 100$ (1/s).

Longitudinal axis vector hodograph $\mathbf{e}_{\xi\eta\zeta}(t)$ was plotted with the help of numerical integration of equations (3), (4) and matrix transformation of components of a unit vector of longitudinal z-axis of main body $\mathbf{e}_{x_1x_2x_3} = (0,0,1)^T$ into initial frame $\xi\eta\zeta$:

$$\mathbf{e}_{\xi\eta\zeta} = [\Psi]^{-1}[\Gamma]^{-1}[\Phi]^{-1}\mathbf{e}_{x_1x_2x_3} \quad (11)$$

$$[\Psi]^{-1} = \begin{bmatrix} 1 & 0 & 0 \\ 0 & \cos \psi & -\sin \psi \\ 0 & \sin \psi & \cos \psi \end{bmatrix}, \quad [\Gamma]^{-1} = \begin{bmatrix} \cos \gamma & 0 & \sin \gamma \\ 0 & 1 & 0 \\ -\sin \gamma & 0 & \cos \gamma \end{bmatrix}, \quad [\Phi]^{-1} = \begin{bmatrix} \cos \varphi & -\sin \varphi & 0 \\ \sin \varphi & \cos \varphi & 0 \\ 0 & 0 & 1 \end{bmatrix}$$

All signs of chaotic motion are shown (fig.2): complexity and irregularity of phase coordinate, broadly distributed power spectrum, positive Lyapunov exponents.

Lyapunov exponents for perturbed motion LOR-gyrostat was calculated on the base of Benettin algorithm [14] (with Gram–Schmidt process of orthogonalization) and have following values (with accuracy 10^{-2}):

$$\begin{aligned} \varepsilon = 0: & \quad \{\bar{\lambda}_1 = 0.89; \bar{\lambda}_2 = 0; \bar{\lambda}_3 = -14.56\}; \\ \varepsilon = 0.1: & \quad \{\lambda_1 = 0.87; \lambda_2 = 0; \lambda_3 = -14.61\}; \\ \varepsilon = 0.5: & \quad \{\lambda_1 = 1.04; \lambda_2 = 0; \lambda_3 = -16.73\}; \\ \varepsilon = 0.75: & \quad \{\lambda_1 = 1.47; \lambda_2 = -0.14; \lambda_3 = -16.71\}; \\ \varepsilon = 0.90: & \quad \{\lambda_1 = 3.66; \lambda_2 = -1.57; \lambda_3 = -13.51\}. \end{aligned}$$

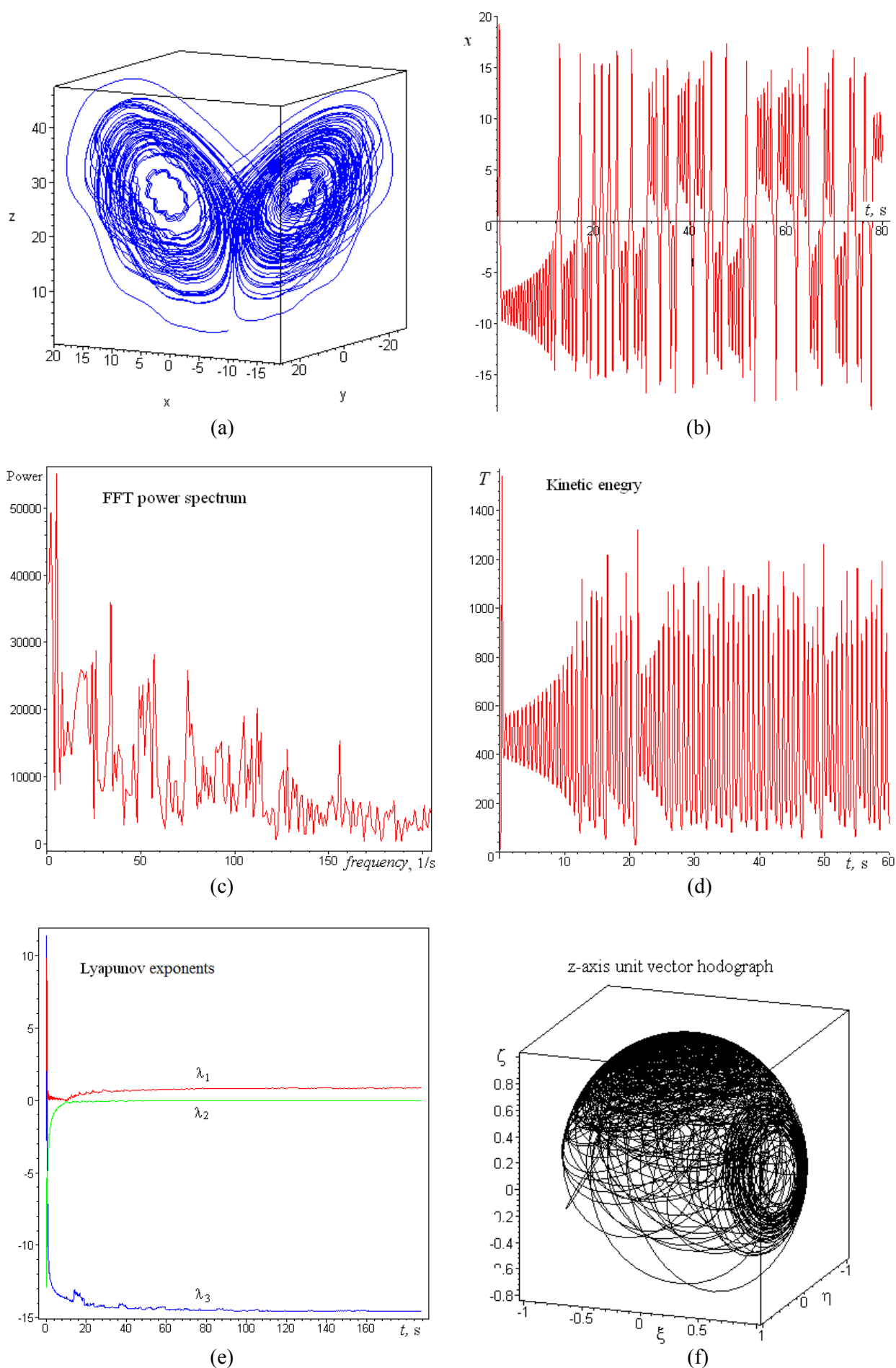


Fig.2 – Numerical research results for LOR-gyrostat with inertia moment variability ($\varepsilon = 0.1$)

The Kaplane-Yorke dimension of perturbed strange attractor increase as compared with classical Lorenz attractor:

$$D_{KY} = D + \frac{1}{|\lambda_{D+1}|} \sum_{j=1}^D \lambda_j; \quad D = \sup i: \sum_{j=1}^i \lambda_j \geq 0; \quad (12)$$

$$D_{KY}|_{\varepsilon=0} \approx D_{KY}|_{\varepsilon=0.1} \approx D_{KY}|_{\varepsilon=0.5} = 2.06; \quad D_{KY}|_{\varepsilon=0.75} = 2.08; \quad D_{KY}|_{\varepsilon=0.90} = 2.15.$$

Calculation of divergence of perturbed system (10) phase flow $\mathbf{F} = [f_x, f_y, f_z]^T$

$$\text{div } \mathbf{F} = -(s + v + 1) \left(1 - \frac{v + 1 - s}{s + v + 1} \varepsilon \sin \Omega t \right) \quad (13)$$

show that the perturbed system is dissipative ($\text{div } \mathbf{F} < 0$) if

$$\varepsilon < |(1 + v + s)/(1 + v - s)| \quad (14)$$

In the classical case of Lorenz ($s = 10; v = 8/3; w = 28$) from condition (14) follow limitation $\varepsilon < 41/19 = 2.16$, which guarantee the system dissipativity at $\varepsilon < 1$. Consequently, every finite (small) the system phase-space volume will reduce to zero value and every phase trajectory will attract to strange attractor.

Comment about application of LOR-case. The Lorenz system, first of all, describes the convective motion of fluid [1]. This system also can be applied to the analysis of dynamos and lasers. In addition it is need to note that LOR-case can, for example, simulate attitude motion of the gyrostat ($\mathbf{R} = [R_1, 0, 0]^T$) with inertia-mass parameters corresponded to a thin disk-shaped body (like a coin: $A = mR^2/2, B = C = mR^2/4$) at presence of propeller blades ($a_{ij} \neq 0$) and roughness of the body surface ($a_{ii} \neq 0$). This makes it possible to apply the LOR-case investigation results to examination of vehicles special motion modes in resistant environments. Also these results can be used for the description of gyrostat-spacecraft perturbed attitude motion with feedback control (interpreting the torques \mathbf{M}_{in}^e as feedback control).

A-gyrostat.

Assume following time-dependencies of inertia moments in the case of A-gyrostat:

$$A(t) = B(t) = A_0(1 + \varepsilon \sin \Omega t); \quad C(t) = A_0(1 - \varepsilon \sin \Omega t) \quad (15)$$

Other parameters in (8.A) are constant. For numerical evaluation we take $\Omega = 100$ (1/s).

Take into account conditions (8.A) and dependencies (15) perturbed motion equations for A-gyrostat can be write as follows:

$$\begin{aligned} \dot{x} &= \frac{2\varepsilon \sin \Omega t}{1 + \varepsilon \sin \Omega t} yz + \frac{y}{1 + \varepsilon \sin \Omega t}; \\ \dot{y} &= -\frac{2\varepsilon \sin \Omega t}{1 + \varepsilon \sin \Omega t} xz + \frac{1}{1 + \varepsilon \sin \Omega t} (yz - x); \\ \dot{z} &= \frac{1}{1 - \varepsilon \sin \Omega t} (1 - y^2). \end{aligned} \quad (16)$$

Lyapunov exponents for perturbed motion of A-gyrostat (with accuracy 10^{-2}):

$$\begin{aligned} \varepsilon = 0: \quad & \{\bar{\lambda}_1 = 0.01; \bar{\lambda}_2 = 0; \bar{\lambda}_3 = -0.01\}; \\ \varepsilon = 0.3: \quad & \{\lambda_1 = 0.03; \lambda_2 = 0; \lambda_3 = -0.03\} \end{aligned}$$

The Kaplane-Yorke dimension in this case always equals to 3; the system is conservative and phase space volume conservation takes place $\left(\sum_{i=1}^3 \lambda_i = 0 \right)$.

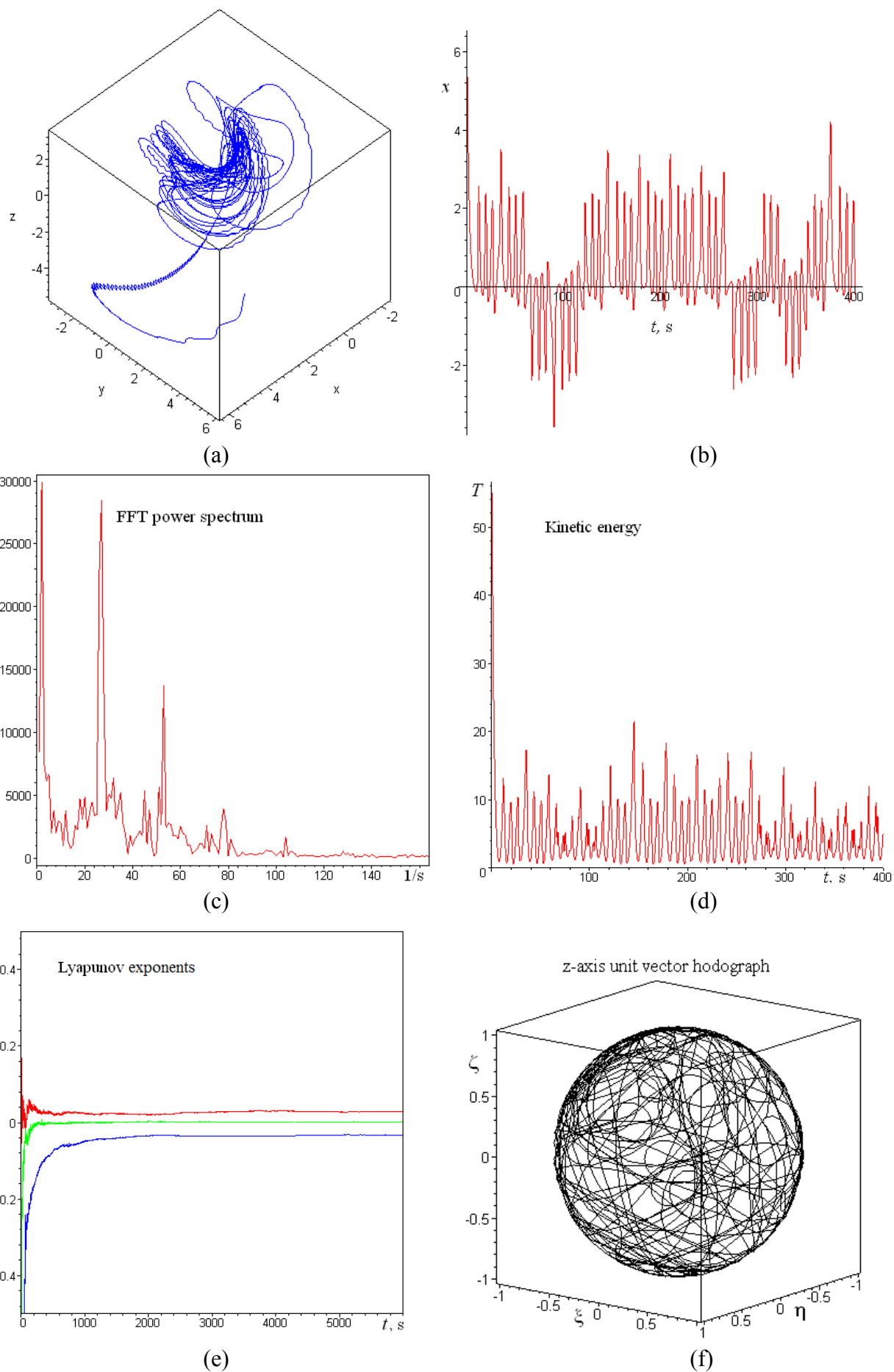


Fig.3 – Numerical research results for A-gyrostatt with inertia moment variability ($\varepsilon = 0.3$)

Integer (not fractional) dimension and presence of positive Lyapunov index means that this system has not strange attractor (like geometry objects with fractional dimension), but gyrostat motion is chaotic (positive λ -exponent mixes of phase trajectories).

Numerical modeling results are presented at figures (fig.3 – fig.6). Fig.4-5 contain Poincaré sections ($z=0$) of the system phase space for unperturbed [4] (fig.4) and perturbed (fig.5, 6) cases. It is needed to note, that phase trajectory intersect the plane ($z=0$) in different region depending on direction of phase point motion along phase trajectory (fig.4-b):

- 1). Region $y \in (-\infty, -1) \cup (1, +\infty)$ corresponds to intersection with direction $\dot{z} < 0$, $z : + \rightarrow -$
- 2). Region $y \in (-1, 1)$ corresponds to intersection with direction $\dot{z} > 0$, $z : - \rightarrow +$

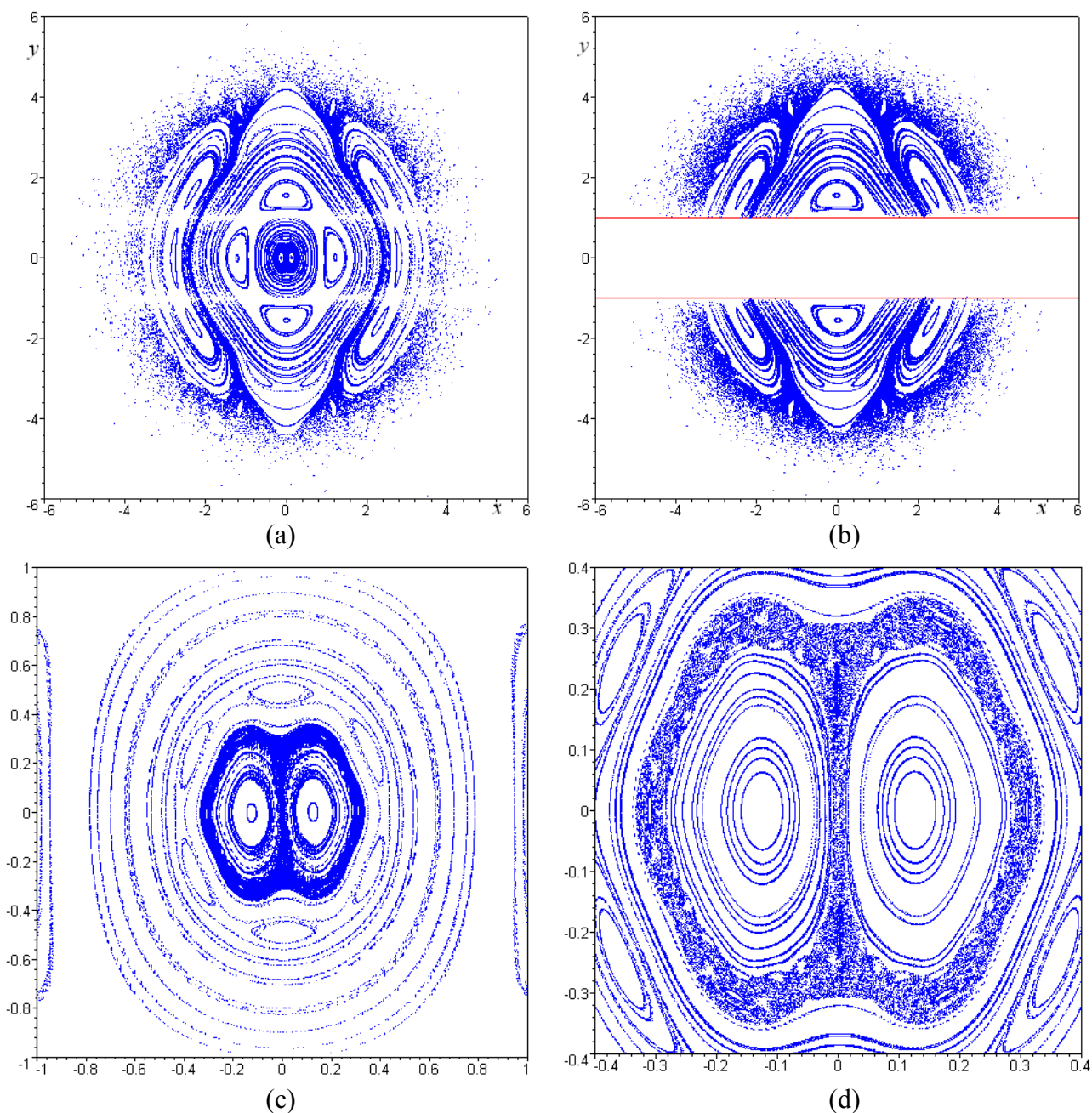


Fig.4 – Poincaré sections ($z=0$) in unperturbed A-gyrostat case ($\varepsilon = 0$) [4]:
 a – general Poincaré section; b – with intersection direction control $z : + \rightarrow -$; c, d - zoom

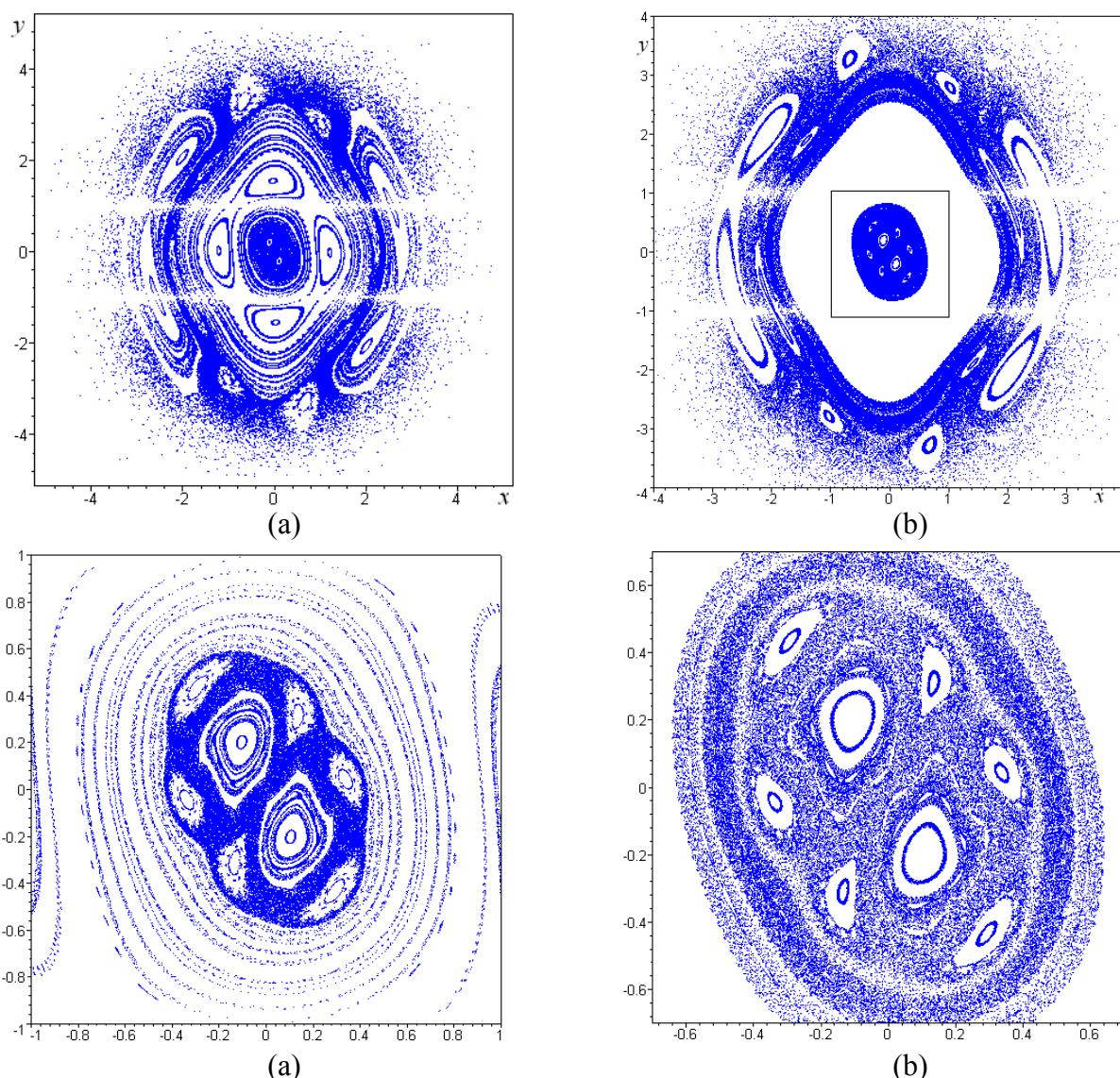


Fig.5 – Poincaré sections ($z=0$) in perturbed A-gyrostator ($\varepsilon=0.3$):
a – general Poincaré section; b – with initial condition from depicted rectangle; c, d - zoom

How can we see, perturbation generate heteroclinic loops and corresponding meander tori at the Poincaré sections (fig. 5). This circumstance even more complicates the system motion dynamics.

Also it is need to note, that time history of kinetic energy $T(t)$ show, on the one hand, gyrostat chaotic motion features and, on the other hand, nonregular characteristics of external environment and internal forces action. Kinetic energy change law imply

$$T = \int (dW^e + dW^i) = W(t) + \text{const}$$

where $W(t)$ is total work of all external (“e”) and internal (“i”) forces. It corroborates the statement that deterministic chaos in dynamical system (and strange attractor like its geometrical image) can be explained on the base of mechanical description: presence of nonregular influence result in nonregular system behavior. Thus, we shall conclude that kinetic energy $T(t)$ time history is also one of the primary technique for examine of chaotic motion.

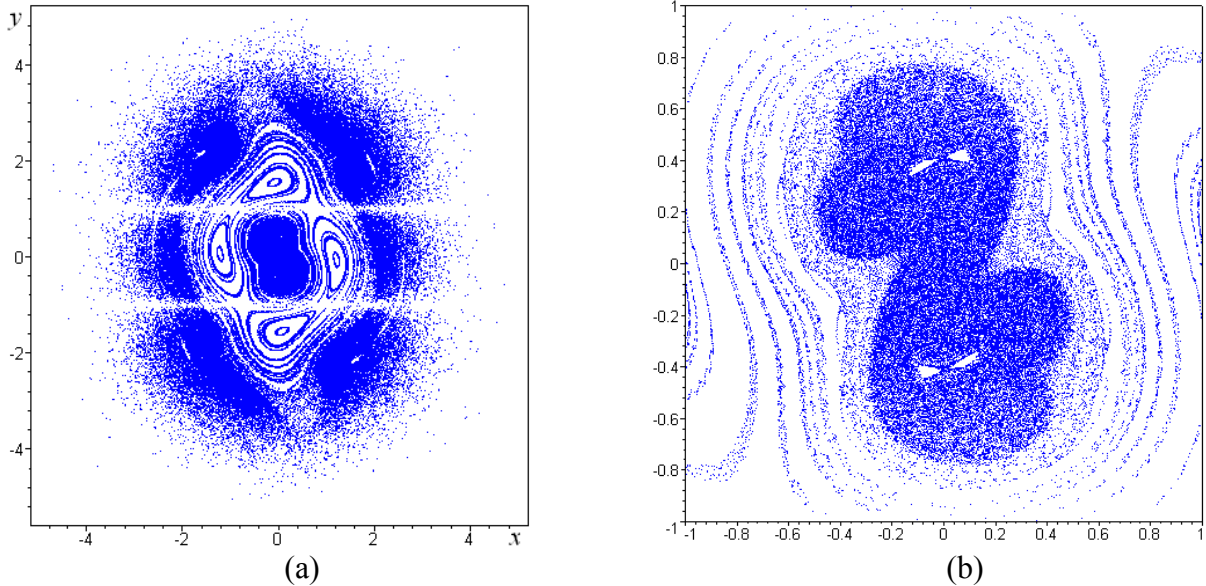


Fig.6 – Poincaré sections ($z=0$) in perturbed A-gyrost ($\varepsilon=0.5$):
 a – general Poincaré section; b – zoom

Comment about application of A-gyrostatt Sprott case. The Sprott system for A-gyrostatt can be applied, for example, to the analysis of attitude motion of the gyrostatt ($\mathbf{R} = [0, 0, R_3]^T$) with inertia-mass parameters of a spherical body ($A=B=C$), xy -propeller blades ($a_{12} = -a_{21} = A + R_3$), smooth body surface ($a_{ii} = 0$) at presence of constant z -spin-up torque ($d_3=A$) and special feedback control ($g_{21}=-b_{32}=A$). This makes it possible to apply the A-case investigation results to examination of gyrostatt-vehicles special motion modes in resistant environments with feedback control.

4.2 Gyrostatt internal rotor angular moment perturbation

Let us investigate of gyrostatt motion at presence of small harmonic perturbations in relative rotor angular moment \mathbf{R} :

$$\mathbf{R} = \tilde{\mathbf{R}}(1 + \varepsilon \sin \Omega t); \quad \tilde{\mathbf{R}} = [R_1, R_2, R_3]^T; \quad R_i = \text{const} \quad (17)$$

This perturbation can be associated with existence of small harmonic disturbances in electric circuit of internal rotor-engine (simulation of simplest self-induction effects). Corresponding motion equations follow from angular moments law:

$$\dot{\mathbf{K}} + \boldsymbol{\omega} \times (\mathbf{K} + \mathbf{R}) = \mathbf{M}_{const}^e + \mathbf{M}_{lin}^e + \mathbf{M}_{quad}^e - \dot{\mathbf{R}} \quad (18)$$

We conduct examination of perturbed motion on the base of NL-gyrostatt. Other type of gyrostatt (A-S, LOR, ROS) can be considered by analogy.

Take into account conditions (8.NL) and (17) perturbed motion equations for NL-gyrostatt will be write as follows:

$$\begin{cases} \dot{x} = -kx + y + wyz + Pert_1 \\ \dot{y} = -x - my + 5xz + Pert_2 \\ \dot{z} = vz - 5xy + Pert_3 \end{cases} \quad (19)$$

where $Pert_i$ are components of vector

$$\mathbf{Pert} = \begin{bmatrix} \frac{\varepsilon}{A} [(R_2 z - R_3 y) \sin \Omega t - R_1 \Omega \cos \Omega t] \\ \frac{\varepsilon}{B} [(R_3 x - R_1 z) \sin \Omega t - R_2 \Omega \cos \Omega t] \\ \frac{\varepsilon}{C} [(R_1 y - R_2 x) \sin \Omega t - R_3 \Omega \cos \Omega t] \end{bmatrix} \quad (20)$$

Let us note, that perturbation vector (20) will be the same also for other type (A-NL).

Case 1. Firstly, consider main case of the NL system with $w=10$. Numerical research results are present at fig.7 and was obtained at following parameters and initial condition values: $A=B=C=1$; $R_1=1$; $R_2=1.5$; $R_3=2$; $\Omega=100$; $\varepsilon=0.01$; $x(0)=0.349$; $y(0)=0.0$; $z(0)=-0.16$.

In this case Lyapunov exponents and Kaplane-Yorke dimension for unperturbed and perturbed motion of NL-gyrostatt (with accuracy 10^{-2}) are equal:

$$\begin{aligned} \varepsilon = 0: & \quad \{\bar{\lambda}_1 = 0.14; \bar{\lambda}_2 = 0; \bar{\lambda}_3 = -0.76\}; \quad D_{KY} = 2.18; \\ \varepsilon = 0.01: & \quad \{\lambda_1 = 0.12; \lambda_2 = -0.01; \lambda_3 = -0.74\}; \quad D_{KY} = 2.18. \end{aligned}$$

Consequently, the system is dissipative (negative sum of all Lyapunov index) and has attractor; the system is chaotic ($\lambda_1 > 0$); the system attractor is strange (fractional D_{KY}).

Case 2. Now consider case with $w=1$; other parameters are the same, like previous case. Numerical research results are present at fig.8.

In this case Lyapunov exponents and Kaplane-Yorke dimension (with accuracy 10^{-2}) are equal:

$$\begin{aligned} \varepsilon = 0: & \quad \{\bar{\lambda}_1 = 0.01; \bar{\lambda}_2 = -0.10; \bar{\lambda}_3 = -0.53\}; \quad D_{KY} = 1.1; \\ \varepsilon = 0.01: & \quad \{\lambda_1 = 0.01; \lambda_2 = -0.11; \lambda_3 = -0.53\}; \quad D_{KY} = 1.09. \end{aligned}$$

The system also is dissipative, chaotic ($\lambda_1 > 0$) and has strange attractor. But absolute value of positive λ_1 -exponent is small (limiting close to zero with actual accuracy), therefore, trajectory mixing is weak. It allows conclude, that the system is quasichaotic. It is also supported by regulation trend of time history of phase coordinate, kinetic energy, longitudinal axes hodograph, and by chaotic but degenerating power spectrum (fig.8).

Case 3. Finally, let us consider case for $w=10$, $v=0$. In this case all Lyapunov exponents are negative and therefore motion is regular, system is dissipative, Kaplane-Yorke dimension equal to zero and attractor is stationary point (corresponded to permanent rotation of main body). The system regular motion represents transition to permanent rotation about body z-axis ($x(t) \rightarrow 0$, $y(t) \rightarrow 0$, $z(t) \rightarrow z^* = \text{const}$). Numerical research results (fig.9) demonstrate signs of regular motion.

Comment about application of NL-gyrostatt case. The Newton-Leipnik system describes attitude motion of spacecraft with linear feedback control [3]. NL-gyrostatt results can be applied to simulation of perturbed attitude nonregular motion of gyrostat-spacecraft.

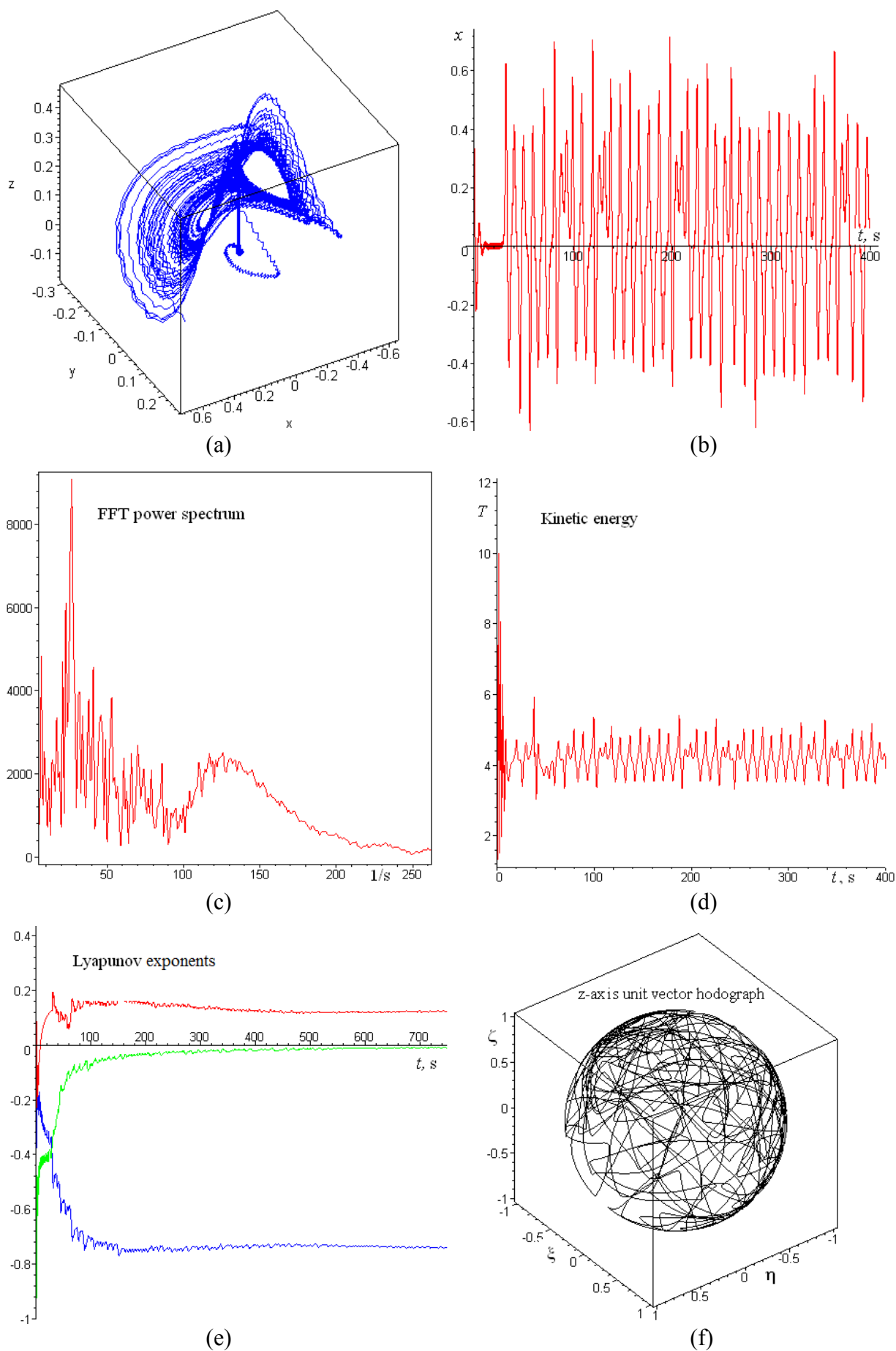


Fig.7 – Numerical research results for NL-gyrostat *chaotic* motion with rotor relative angular moment variability ($\varepsilon = 0.01$, $w = 10$)

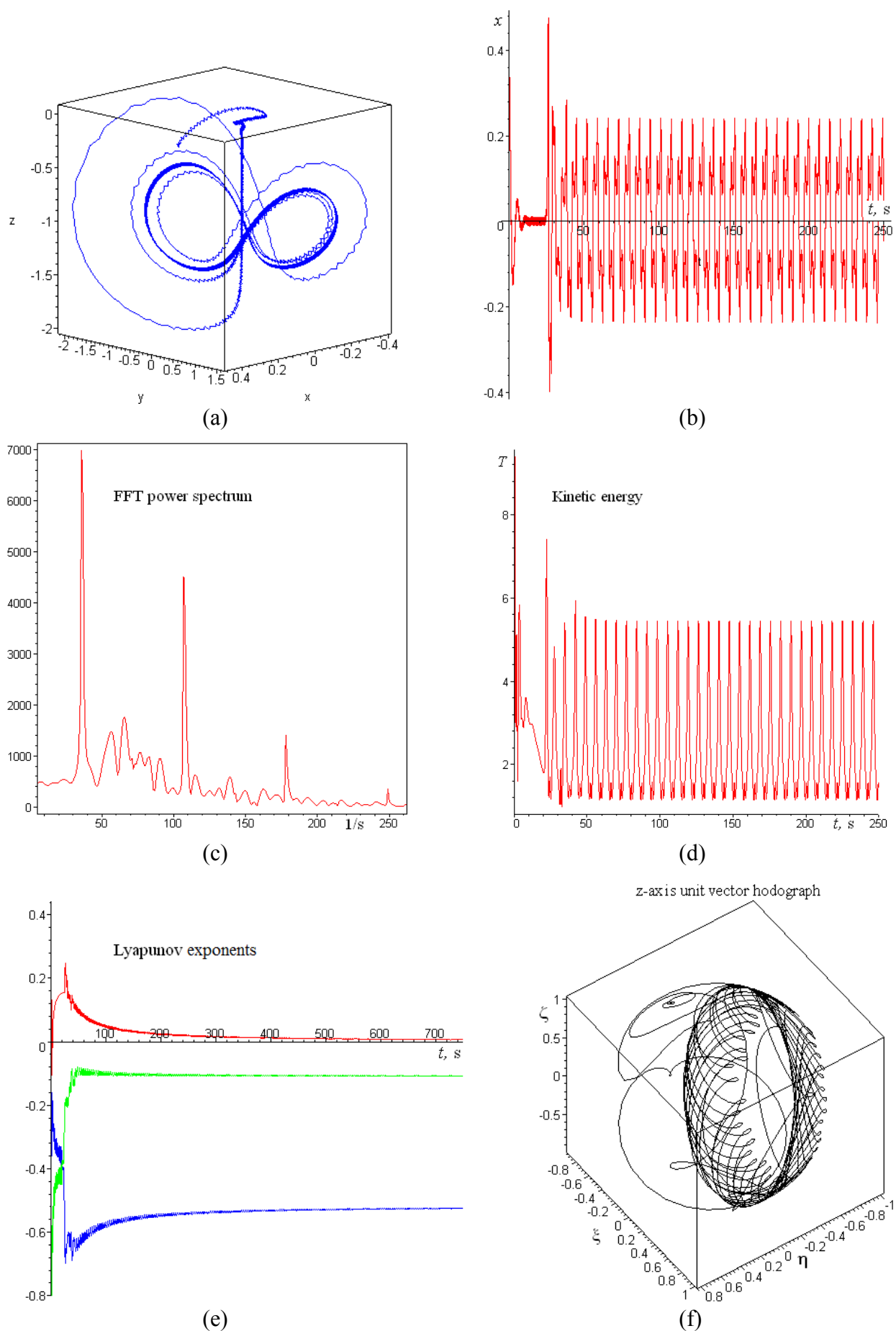


Fig.8 – Numerical research results for NL-gyrostat *quasichaotic* motion with rotor relative angular moment variability ($\varepsilon = 0.01$, $w = 1$)

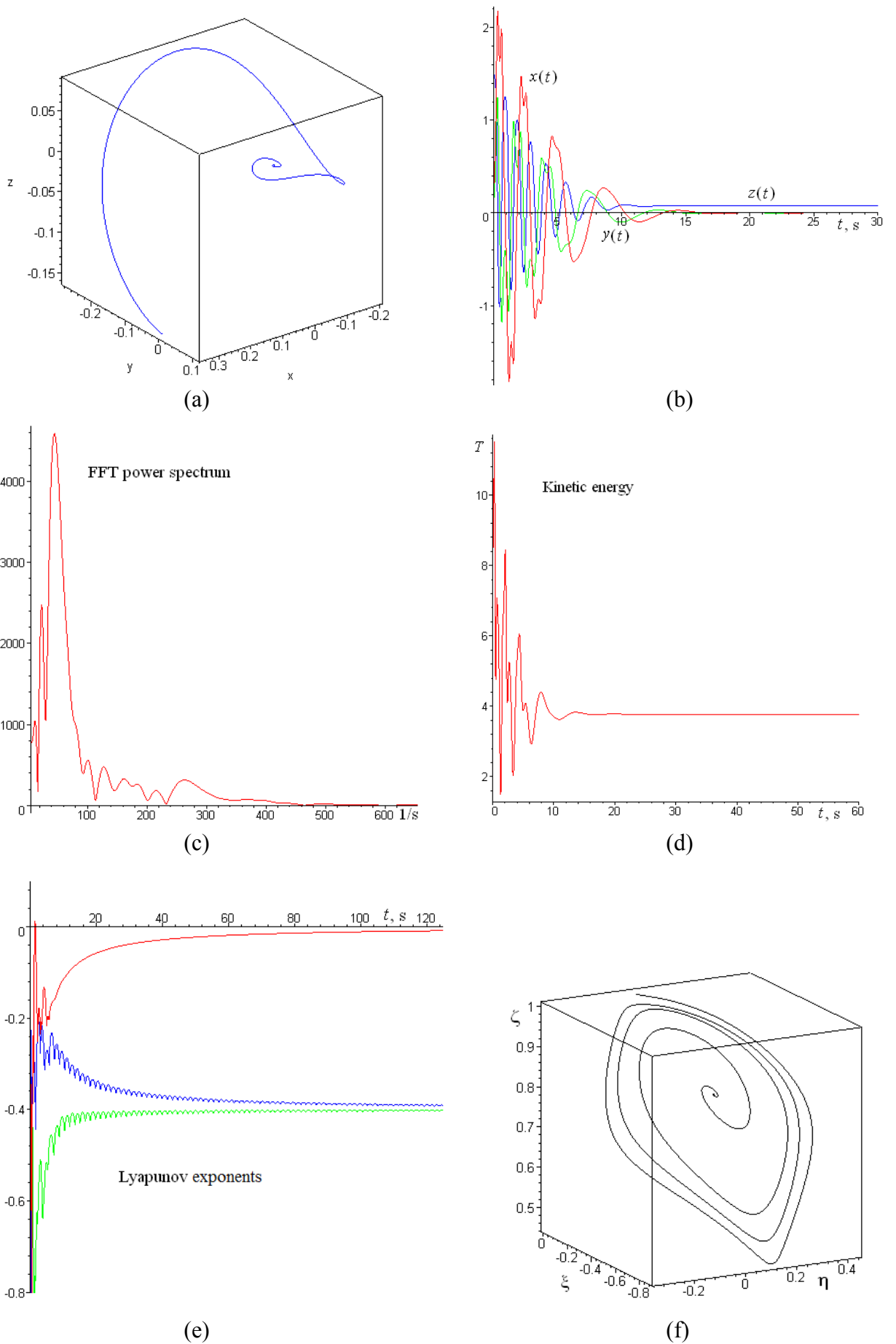


Fig.9 – Numerical research results for NL-gyrostat *regular* motion ($\varepsilon=0$, $w=1$, $\nu=0$)

5 Conclusion

Links between mathematical models of gyrostats and dynamical systems with strange attractors (Lorenz, Rössler, Newton-Leipnik and Sprott systems) were established. In order to examine of perturbed motion several numerical techniques was used: time-history of phase coordinate, kinetic energy, power spectrum of fast Fourier transformation, asymptotics of Lyapunov exponents and gyrostat longitudinal axis vector hodograph, and Poincaré sections. Mentioned numerical techniques showed chaotic and quasichaotic behavior of motion. Cases for perturbed gyrostat motion with variable periodical inertia moments and with periodical internal rotor relative angular moment were considered.

Acknowledgments

Russian Federation Presidential Program for scientists and leading scientific schools (MK-1497.2010.8) supported this work. Also author is thankful to government program of expansion of national research university (S.P.Korolev Samara State Aerospace University).

References

- [1] E. N. Lorenz, Deterministic nonperiodic flow, *J. Atmos. Sci.* 20 (1963) 130–141.
- [2] O. E. Rössler, An equation for continuous chaos, *Phys. Lett. A* 57 (1976) 397–398.
- [3] R. B. Leipnik, T. A. Newton, Double strange attractors in rigid body motion with linear feedback control, *Phys. Lett A* 86 (1981) 63-67.
- [4] J. C. Sprott, Some simple chaotic flows, *Phys. Rev. B* 50 (1994) R647–R650.
- [5] J. C. Sprott, Simplest dissipative chaotic flow, *Phys. Lett. A* 228 (1997) 271-274.
- [6] A. V. Borisov, I. S. Mamaev, Dynamics of the Rigid Body. *Izhevsk. RCD.* 2001. P. 384. In Russian.
- [7] M. Inarrea, V. Lanchares, Chaotic pitch motion of an asymmetric non-rigid spacecraft with viscous drag in circular orbit, *Int. J. Non-Linear Mech.* 41 (2006) 86–100.
- [8] X. Tong, B. Tabarrok, F.P.J. Rimrott, Chaotic motion of an asymmetric gyrostat in the gravitational field, *Int. J. Non-Linear Mech.* 30 (3) (1995) 191–203.
- [9] J. Kuang, S. Tan, K. Arichandran, A.Y.T. Leung, Chaotic dynamics of an asymmetrical gyrostat, *Int. J. Non-Linear Mech.* 36 (2001) 1213-1233
- [10] A. V. Doroshin, Analysis of attitude motion evolutions of variable mass gyrostats and coaxial rigid bodies system, *Int. J. Non-Linear Mech.* 45 (2010) 193–205.
- [11] A.P.M. Tsui, A.J. Jones, The control of higher dimensional chaos: comparative results for the chaotic satellite attitude control problem, *Physica D* 135 (2000) 41–62.
- [12] L. Zhou, Y. Chen, F. Chen, Stability and chaos of a damped satellite partially filled with liquid, *Acta Astronautica* 65 (2009) 1628-1638.
- [13] J. Baek, Adaptive fuzzy bilinear feedback control design for synchronization of TS fuzzy bilinear generalized Lorenz system with uncertain parameters, *Physics Letters A* 374 (2010) 1827–1834.
- [14] G. Benettin, L. Galgani, A. Giorgilli, J.-M. Strelcyn, Lyapunov characteristic exponents for smooth dynamical systems and for Hamiltonian systems: A method for computing all of them. P.I: Theory. P.II: Numerical application, *Meccanica* 15 (1980) 9-30.